*Stanford Exploration Project, Report 77, November 17, 1997, pages 389–406*

*Stanford Exploration Project, Report 77, November 17, 1997, pages 389–406*

# Modeling in polar coordinates using one way wave equations

*Dave Nichols*[1]

***keywords:*** *velocity, modeling, graphics, phase, algorithm*

**ABSTRACT**

Mono-frequency Green's functions can be calculated using several frequency domain algorithms. I model the response to a point impulse in 2-D using phase shift, PSPI and $\omega - x$ implicit finite difference algorithms. All of these algorithms can be implemented in both rectangular and polar coordinates. In polar coordinates an outgoing wavefield can be accurately modeled using a low dip algorithm. This means that high dip accuracy can be obtained at low dip cost.

## INTRODUCTION

Many geophysical processes can be formulated in terms of the Green's functions of the wave equation. However, these formulae are usually transformed into other forms before they are implemented. The reason for this is the prohibitive cost of calculating all the required solutions. A process like prestack migration requires the calculation of the Green's function for every surface (source or receiver) location.

One common way to overcome this problem is to use an asymptotic form of the solution. These are usually of the form $Ae^{-\omega\tau}$ where $\tau$ can be found by solving the eikonal equation and $A$ can be found by solving the transport equation. These solutions are valid when wavelength of the velocity variations in the medium is much greater than the wavelength of the seismic data. Even when the scale of medium variation is large compared to the seismic wavelength, there are still problems associated with this approach. When there are multiple arrivals present in the data, calculating all the arrivals can become complicated. Many implementations calculate only the first arriving events. In particular, finite difference solutions to the eikonal equation can calculate the first arrivals efficiently, but they do not model the later arrivals. However, if the first arrival contains little energy, the solution obtained will be a poor approximation of the total Green's function.

[1]**email:** not available

In this paper I examine some methods for obtaining mono-frequency Green's functions. The complete Green's function is the superposition of all the mono-frequency Green's functions. Using currently available computers, it may be too expensive to routinely calculate these functions for all frequencies. However, this is likely to change rapidly. In addition, it may be informative to just compute a few Green's functions at selected frequencies and examine their dependence on frequency.

I use one-way extrapolators to downward or outward continue an initial condition until a solution is obtained in the whole space of interest. The one-way equations do not represent the full Green's function. However, they contain the information that is usually of greatest interest, the amplitude and phase of the primary arrivals. Arrivals due to multiple reflections may not be present, but these are often undesirable in geophysical applications. The multiply scattered events are very sensitive to the velocity model. If the model is not known accurately it can be beneficial to ignore multiples in the calculation of the Green's functions.

I show how to generate the Green's functions in a polar coordinate frame. Polar coordinates have been successfully used in finite difference travel time estimation (van Trier and Symes, 1991). They have the advantage of providing a coordinate frame that matches the constant velocity wavefronts. Even in variable velocity models, this results in wave propagation at low angles to the coordinate frame. Use of the polar coordinates could be regarded as a step towards using Gaussian beams (Červený et al., 1982). However, I feel that polar coordinates give many of the advantages of Gaussian beams without requiring a ray-tracing step to define the local coordinate frame.

## RECTANGULAR COORDINATES

In a 2-D rectangular coordinate frame the wave equation in the time domain is given by,

$$\frac{\partial^2 P}{\partial z^2} + \frac{\partial^2 P}{\partial x^2} = \frac{1}{v^2}\frac{\partial^2 P}{\partial t^2}$$

When this equation is Fourier transformed over time and $x$ we obtain,

$$\frac{\partial^2 P}{\partial z^2} - k_x^2 P = -\frac{\omega^2}{v^2} P$$

or,

$$\frac{\partial^2 P}{\partial z^2} = \left[k_x^2 - \frac{\omega^2}{v^2}\right] P$$

If we assume a solution of the form,

$$P(z) = P(z_0) e^{ik_z (z - z_0)},$$

we find

$$k_z = \pm\sqrt{\frac{\omega^2}{v^2} - k_x^2}. \tag{1}$$

Given a solution at one depth level $P(z)$ we can extrapolate it to a new depth level using a pure phase shift $P(z+\Delta z) = P(z)e^{ik_z \Delta z}$. The positive square root is chosen for positive frequencies in order to select waves that propagate downwards as time increases.

Using this method we can propagate an initial condition specified at $z = 0$ to any depth by applying suitable phase shifts at each depth level.

### Initial conditions in rectangular coordinates

For surface seismic experiments we require Green's functions that are the response to an impulse at a single point on the surface. However the phase shift algorithm requires initial conditions at all locations on the surface,$P(\omega, x, z = 0)$. Since horizontal waves, reflected waves, and overturned waves can all contribute to the surface wavefield it appears that you must have already modeled the data in order to find the initial condition. To avoid this problem I calculate a dip limited Green's function so that only events traveling at less than some angle to the vertical (say 80 degrees) are propagated. I assume that none of this energy reaches the surface. The initial condition is then just an impulse at the source location that is dip filtered to an appropriate dip range. While this does not calculate the Green's function correctly at high dips, it should be adequate for the dip ranges typical in seismic data.

Figure 1 shows the amplitude and phase plots for a mono-frequency Green's function calculated for a constant velocity medium. The amplitude should be radially symmetric but it decays near the surface because of the dip limitation. Figure 2 shows one time slice through the full Green's function in the $(x, z, t)$ domain. This was calculated by inverse transforming a complete set of mono-frequency Green's functions. The dip limitation in the initial conditions is clearly visible as an amplitude decay of the wavefront at steeper angles.

Because the simple one-way equation only propagates energy downwards, it cannot correctly model overturned waves. Claerbout (1985) explained how to overcome this problem by saving the upgoing energy at each depth step, and then use an upwards extrapolation phase to pick up the upgoing energy and propagate it to the surface. This method of modeling overturned waves clearly requires twice as much computation as a simple downward extrapolation.

## POLAR COORDINATES

The problems associated with overturned waves and initial conditions can be overcome by calculating the Green's functions in polar coordinates. Van Trier and Symes (1991) use polar coordinates for similar reasons in their finite difference solution to the eikonal equation.

I will follow exactly the same steps in deriving the algorithms in polar coordinates

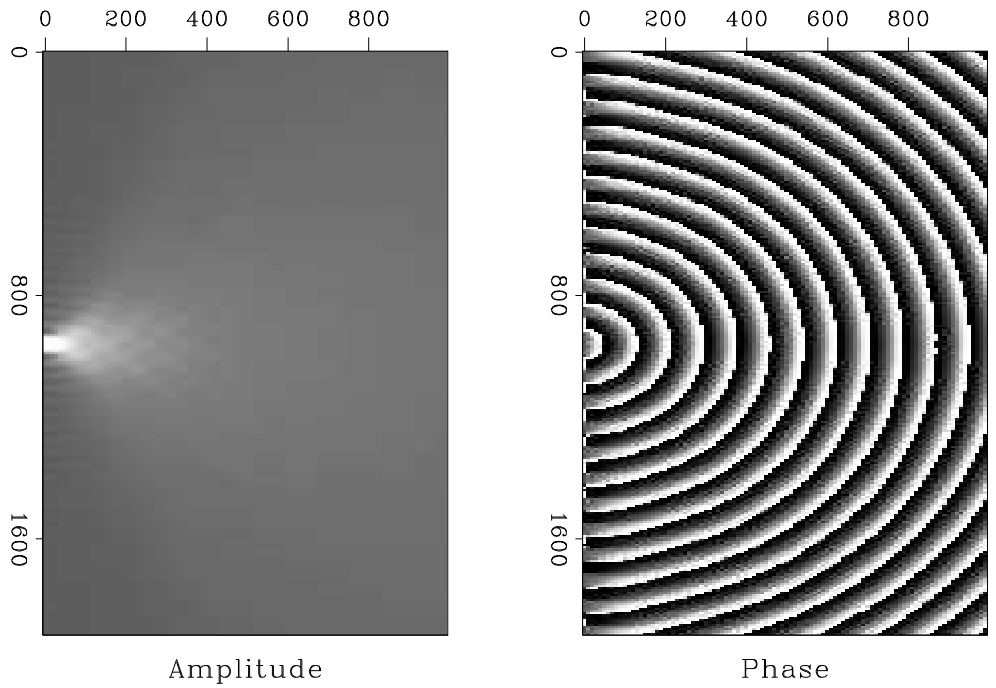


Figure 1: Amplitude (left) and phase (right) for a mono-frequency Green's function calculated in rectangular coordinates. This is a constant velocity medium with a dip filtered impulse as the initial condition. dave2-rect-one [CR]

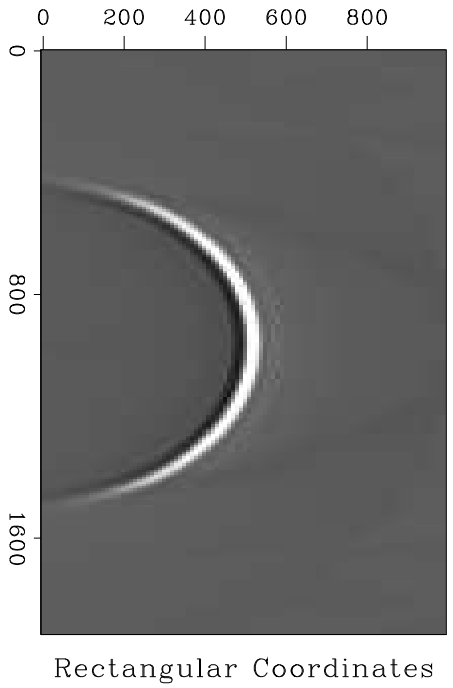


Figure 2: A time slice through the (x,z,t) Green's function calculated by inverse transforming a complete range of mono-frequency Green's functions calculated in rectangular coordinates. dave2-rect-all [CR]

as I did in rectangular coordinates. In a 2-D polar coordinate frame, the wave equation is,

$$\frac{\partial^2 P}{\partial r^2} + \frac{1}{r}\frac{\partial P}{\partial r} + \frac{1}{r^2}\frac{\partial^2 P}{\partial \theta^2} = \frac{1}{v^2}\frac{\partial^2 P}{\partial t^2}$$

When this equation is Fourier transformed over time and $\theta$ we obtain,

$$\frac{\partial^2 P}{\partial r^2} + \frac{1}{r}\frac{\partial P}{\partial r} - \frac{1}{r^2}k_\theta^2 P = -\frac{\omega^2}{v^2}P$$

If we assume a solution of the form,

$$P(r) = P(r_0)e^{ik_r(r-r_0)}, \tag{2}$$

we find,

$$k_r = \frac{i}{2r} \pm \sqrt{\frac{\omega^2}{v^2} - \frac{k_\theta^2}{r^2} - \frac{1}{4r^2}}$$

Thus given a wavefield at some radius $r$ we can propagate it to a new radius using,

$$P(r+\Delta r) = P(r)e^{-\frac{\Delta r}{2r}}e^{i\sqrt{\frac{\omega^2}{v^2}-\frac{k_\theta^2}{r^2}-\frac{1}{4r^2}}\Delta r}$$

The real part of this expression controls the amplitude decay due to increasing wavefront radius and the imaginary part gives the phase shift.

The initial conditions are not supplied at $r = 0$, but rather at some finite initial radius $r_0$. The region between the origin and $r_0$ is assumed to be homogeneous. A suitable initial condition is,

$$P(r_0, \theta, \omega) = \frac{1}{\sqrt{r_0}}\frac{1}{\sqrt{\omega}}e^{i\omega\frac{r_0}{v}}.$$

Figure 3 shows the amplitude and phase plots for a mono-frequency Green's function calculated for a constant velocity medium. The polar coordinate data has been re-interpolated onto the same rectangular grid as the rectangular coordinate data. The amplitude is now more uniform for all dips. Figure 4 shows one time slice through the full Green's function in the $(x, z, t)$ domain. The result is a much more accurate representation of the wavefront.

## LATERAL OR ANGULAR VELOCITY VARIATION

The two phase shift schemes are suitable for use with a constant velocity model or a model which varies only in the direction in which the data is extrapolated. For rectangular coordinates this is a $v(z)$ model, and for polar coordinates it is a $v(r)$ model. When the velocity model is not of a suitable form, a more complicated algorithm must be used.

In many cases a $v(z)$ model is geologically reasonable, but this is rarely true of a $v(r)$ model. One disadvantage of working in polar coordinates is that the simple phase shift algorithm cannot be used for a $v(z)$ model.

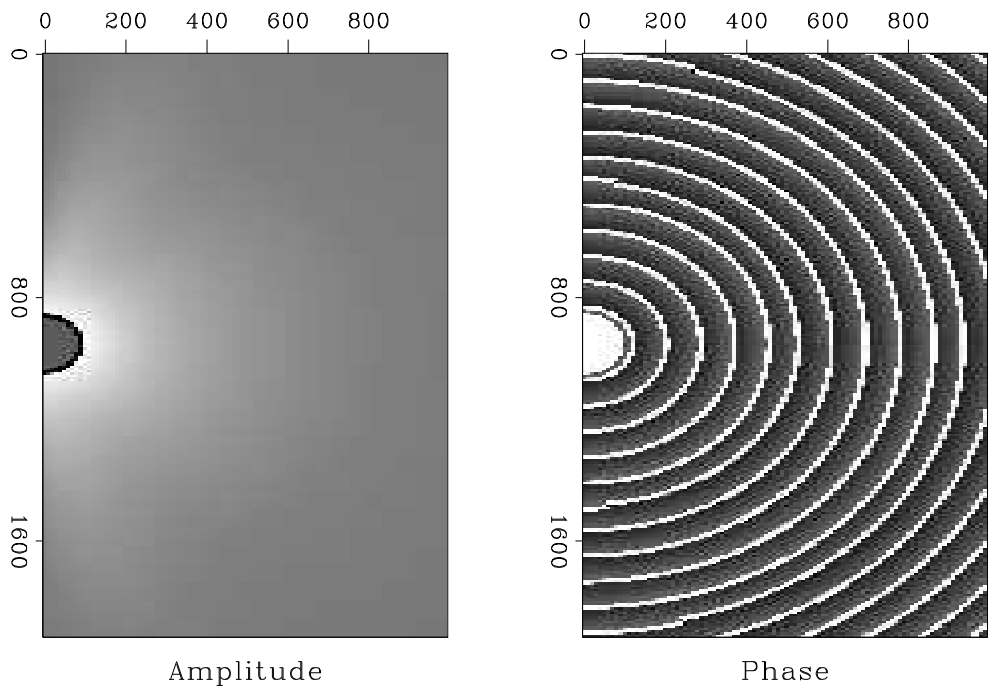


Figure 3: Amplitude (left) and phase (right) for a mono-frequency Green's function calculated in polar coordinates. The initial condition is a constant value on a semi-circle of radius 80m. dave2-pol-one [CR]

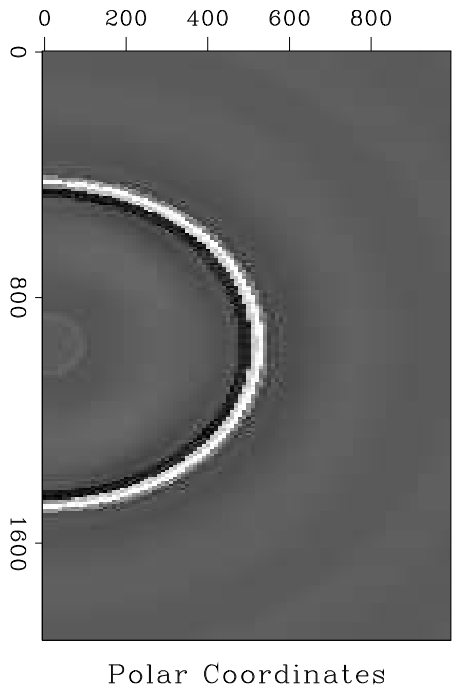


Figure 4: A time slice through the (x,z,t) Green's function calculated by inverse transforming a complete range of mono-frequency Green's functions calculated in polar coordinates. dave2-pol-all [CR]

### Phase shift plus interpolation

The simplest extension to the phase shift algorithm is "phase shift plus interpolation" (PSPI) (Gazdag and Sguazzero, 1984). This algorithm approximates the extrapolation of the wavefield in a spatially varying velocity field by interpolating the results of a set of constant velocity extrapolations. The interpolation is performed in the space domain. This method therefore requires an inverse Fourier transform of each constant velocity panel back to the space domain ($x$ or $\theta$), and a forward transform of the interpolated result to the wavenumber domain, for each extrapolation step in $z$ or $r$.

I use the simplest form of the PSPI algorithm which uses only two constant velocity extrapolations. The two velocities are the maximum and minimum velocity at the current depth or radius.

In rectangular coordinates,

$$\begin{aligned}
P_1(z+\Delta z,k_x) &= P(z,k_x)e^{ik_z(v_{min},k_x)\Delta z} \\
P_2(z+\Delta z,k_x) &= P(z,k_x)e^{ik_z(v_{max},k_x)\Delta z} \\
P_1(z+\Delta z,x) &= \mathcal{FT}_x^{-1}\left\{P_1(z+\Delta z,k_x)\right\} \\
P_2(z+\Delta z,x) &= \mathcal{FT}_x^{-1}\left\{P_1(z+\Delta z,k_x)\right\} \\
P(z+\Delta z,x) &= P_1(z+\Delta z,x)\frac{v_{max}-v(x)}{v_{max}-v_{min}} + P_2(z+\Delta z,x)\frac{v(x)-v_{min}}{v_{max}-v_{min}} \\
P(z+\Delta z,k_x) &= \mathcal{FT}_x\left\{P(z+\Delta z,x)\right\}
\end{aligned}$$

In polar coordinates the algorithm has the same form with $r$ replacing $z$.

Figure 5 shows the results of modeling in a medium which has a linear gradient in $x$ and $z$. The velocity field in this model is $v(x,z) = v_0 + \alpha(x-x_0) + \beta(z-z_0)$. The plot on the left is computed in a rectangular coordinates and the one on the right in polar coordinates. They both show an asymmetric wavefront produced by the velocity gradient The polar coordinate result contains energy at higher dips that the rectangular coordinate result because it does not start with a dip filtered impulse.

### Paraxial approximations

The most common way of extrapolating the wavefield in a variable velocity medium is to use a paraxial approximation to the wave equation. The well known 45° paraxial approximation to equation (1) is,

$$\frac{\partial P}{\partial z} = i\frac{\omega}{v}P - \frac{\frac{iv}{2\omega}\frac{\partial^2}{\partial x^2}}{1+\frac{v^2}{4\omega^2}\frac{\partial^2}{\partial x^2}}P$$

Using the usual splitting procedure this becomes,

$$(1-\frac{v^2}{4\omega^2}\frac{\partial^2}{\partial x^2})\frac{\partial Q}{\partial z} = \frac{iv}{2\omega}\frac{\partial^2 Q}{\partial x^2}$$

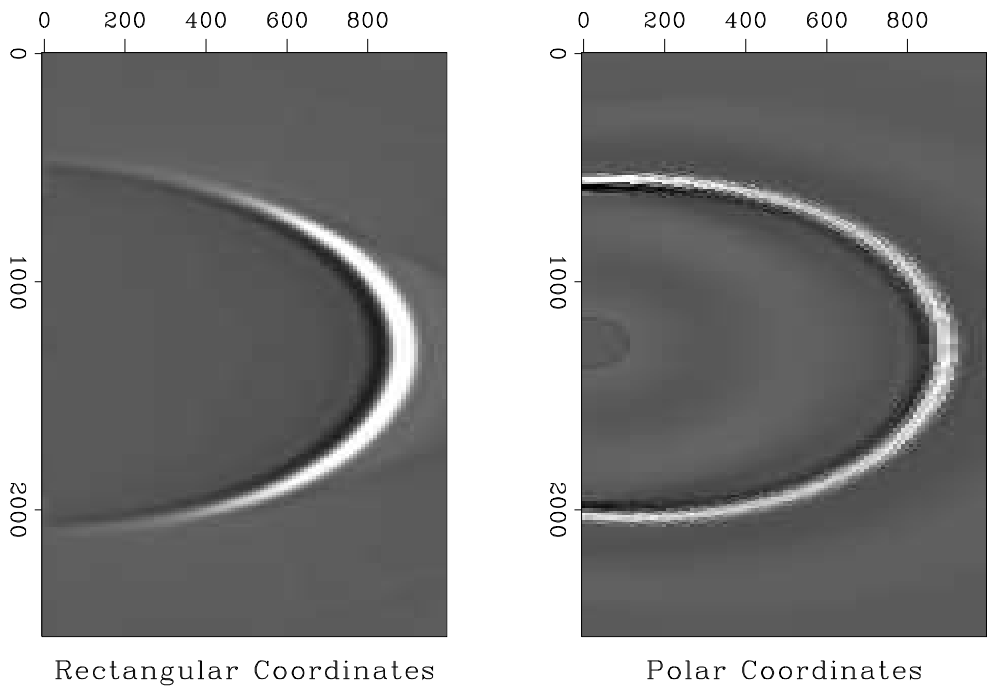


Figure 5: A time slice from modeling in a linear gradient medium. The velocity field has a gradient of 5 $(ms^{-1})/m$ in depth and 5 $(ms^{-1})/m$ in $x$. The result on the left is computed in rectangular coordinates, the one on the right is computed in polar coordinates. dave2-grad-both [CR]

followed by,

$$P(z+\Delta z) = exp(i\int \frac{\omega}{v}\Delta z)Q(z+\Delta z).$$

Discretization of the first equation using the Crank-Nicholson scheme results in a tridiagonal set of equations to be solved in order to propagate the wavefield from a level $z$ to $z+\Delta z$.

The equations in polar coordinates can be similarly transformed, the paraxial approximation is,

$$\frac{\partial P}{\partial r} = \left(\frac{-1}{r^2} + i\sqrt{\alpha}\right) P - \frac{\frac{i\sqrt{\alpha}}{2r^2}\frac{\partial^2}{\partial\theta^2}}{1-\frac{\alpha}{4r^2}\frac{\partial^2}{\partial\theta^2}}P$$

where,

$$\alpha = \sqrt{\frac{\omega^2}{v^2} - \frac{1}{4r^2}}$$

After splitting this becomes,

$$(1-\frac{\alpha}{4r^2}\frac{\partial^2}{\partial\theta^2})\frac{\partial Q}{\partial r} = \frac{i\sqrt{\alpha}}{2r^2}\frac{\partial^2 Q}{\partial\theta^2}$$

followed by,

$$P(r+\Delta r) = exp\left(\frac{-1}{r^2} + i\sqrt{\alpha}\Delta r\right) Q(r+\Delta r)$$

Again discretization of the first equation yields a tridiagonal set of equations to be solved for each depth step.

The results of using these two schemes in a constant velocity space are shown in figure 6. The 45° approximation is clearly visible in the rectangular coordinate data. Because the wavefront propagates at zero degrees to the polar coordinate frame, the polar data does not show any artifacts due to the 45° approximation.

Paraxial approximations will not accurately model events that propagate at high angles to the coordinate frame of the finite difference mesh. In rectangular coordinates this means that near vertical waves should be propagated using depth extrapolation, and near horizontal waves would be best modeled using $x$-extrapolation. If the problem to be solved is one of downward continuing surface data that contains events that are mostly near vertical (e.g. zero offset migration), a rectangular coordinate frame and depth extrapolation are appropriate. On the other hand if the problem is one of modeling a near circular outgoing wavefront from a point source, then polar coordinates and outward radial extrapolation are superior.

## PROBLEMS WITH POLAR COORDINATES

The major disadvantage of using a polar coordinate frame is that it is only suitable for calculating the Green's function for a single point. When Green's functions are to

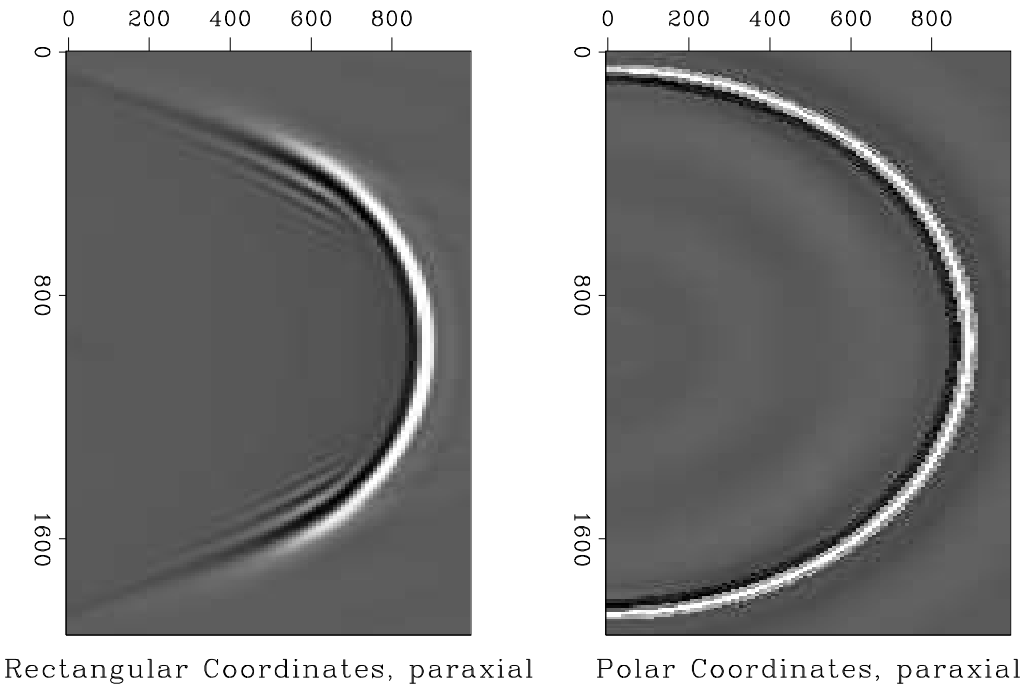


Figure 6: Modeling in a constant velocity medium using the 45° paraxial approximation. The plot on the left was computed in rectangular coordinates the plot on the right was computed in a polar coordinate frame. dave2-parax-both [CR]

be combined, they must be interpolated to a common coordinate frame. In contrast, data from rectangular coordinate frames centered at different points can be combined by a simple shift along the coordinate axes.

All of the polar coordinate figures in this paper have been interpolated onto the same mesh as the rectangular coordinate frame data using a bilinear interpolator. In some figures, the artifacts produced by the interpolation step are clearly visible. The polar data has a "rough" quality that the rectangular coordinate data does not. The problem is most severe when the radius is large. In these cases the spacing between the different radii is much larger than the largest spacing on the rectangular grid. In these regions aliasing may become a problem if the waves propagate at an high angle to the polar grid.

Another problem is that the trial solution used in equation (2) is only an approximate solution. It is only valid in the far field and breaks down at low frequency and small radius. This can be seen from the formula for the radial wavenumber,

$$k_r = \frac{i}{2r} \pm \sqrt{\frac{\omega^2}{v^2} - \frac{k_\theta^2}{r^2} - \frac{1}{4r^2}}$$

The expression inside the square-root becomes negative for all values of $k_\theta$ when $\frac{1}{4r^2} > \frac{\omega^2}{v^2}$. This provides a lower limit to the radius at which to specify the initial condition $r > \lambda/2$. In practice it is advisable to make the initial radius a least two

wavelengths of the lowest frequency.

### More complicated coordinate frames

The principal advantage of polar coordinates is that the computational grid is a better match to the wavefront than a rectangular grid. Because of this we are able to obtain high dip (in the rectangular frame) accuracy with a 45° extrapolator. This principle could be carried further.

In a $v(z)$ medium we could use a grid that followed $v(z)$ raypaths, instead of straight radial lines, and had a second coordinate that was along contours of equal traveltime. In this medium, if we had chosen the correct velocity, the wavefront would always conform to the grid and a low angle extrapolator could be used. There are disadvantages to this coordinate system, the wave equation becomes even more complicated, and the derivatives in "$r$" and "$\theta$" are not decoupled as they are in the polar system. The tradeoff to be made is between having a more complicated wave equation and being able to use a lower accuracy paraxial approximation.

In a general velocity medium we could use a local coordinate system that followed all the rays and then use a zero degree extrapolator to propagate the energy. This would be something very close to the method of Gaussian beams (Červený et al., 1982). One disadvantage of Gaussian beams is that the energy always propagates along the asymptotic ray. In contrast when using a paraxial wave equation, whatever coordinate system you choose, you allow energy to propagate at an angle to the coordinate system. In a geometrically dispersive medium the asymptotic ray may not be the true "ray" at low frequencies (Biondi, 1992). Using of a paraxial wave equation allows the energy to take different paths at different frequencies.

Another consideration when using Gaussian beams is that you must trace the rays for all the events that you wish to contribute to your model. If you which the model to contain reflection or diffraction energy you must trace rays corresponding to those wavefronts. This could be regarded as an advantage, at least you get to choose which events are contained in your model. However the polar coordinate system requires no ray tracing at all and for many velocity models a 45° wave equation on the polar grid will propagate all events of interest accurately.

In general I feel that the greatest jump in quality comes from the change from rectangular coordinates to polar coordinates. Further refinements may be more effort than they are worth. However, this is obviously a subject worthy of further investigation.

## SOME EXAMPLES

Figure 7 shows the modeling results for a $v(z)$ medium with a strong velocity gradient ($10ms^{-1}/m$). In this medium the wavefronts overturn. The rectangular coordinate

modeling code does not model these waves because the wavefield is always extrapolated downwards and any energy in the evanescent zone (with a dip greater than 90° ) is removed at each downwards extrapolation step. However it is surprising to see energy in the rectangular coordinate frame that is apparently upgoing. This is a byproduct of the high velocity gradient, the energy has a phase slowness that points horizontally but a group slowness that points upwards. There is less energy in the "overturned" region that there should be, because the true overturned energy has not been modeled. The two polar coordinate frames show the correct amount of overturned energy. In this particular example the 45° result may be better that the PSPI result in polar coordinates. This is because the very strong gradient is not well handled by the PSPI algorithm. The gradient affects the polar coordinate PSPI code because there is a strong gradient in $\theta$, even though there in no gradient in $x$.

Figure 8 shows another result with upgoing energy. In this case the energy may not be desirable. The model is a two layer medium with a step function in velocity at 300m. The rectangular coordinate frame phase shift result shows only downgoing waves. In contrast the two polar coordinate results display a small piece of reflected energy. This is energy that is upgoing, but still outgoing! Once the angle of incidence exceeds 45° to the vertical the reflected energy is propagated outwards in the polar coordinate frame. There is also some dispersed energy in the 45° result. This is probably due to reflected energy that travels at more than 45° to the polar grid and is thus poorly modeled.

Figure 9 shows the result of modeling in a medium with a small low velocity anomaly. The anomaly is a Gaussian blob with a half width of 100m. Apart from the loss of high dips in the rectangular coordinate frame, all three methods produce similar results. The main difference is that the 45° $\omega - x$ method was much cheaper to produce.

## CONCLUSIONS

Mono-frequency Green's functions can be computed using phase shift or finite-difference schemes in either rectangular or polar coordinates. In polar coordinates the 45° $\omega - x$ approximation will give accurate high dip results at low dip cost. The $\omega - x$ domain method also handles laterally variable velocity more robustly than the PSPI method that is required for high dip accuracy in rectangular coordinates.

## REFERENCES

Biondi, B., 1992, Solving the frequency-dependent Eikonal equation: 62nd Ann. Internat. Mtg., Soc. Expl. Geophys., Expanded Abstracts, 1315–1319.

Červený, V., Popov, M. M., and Psenćik, I., 1982, Computation of wave fields in inhomogenous media: Geophys. J. Roy. Astr. Soc., **70**, 109–128.

Claerbout, J. F., 1985, Tuning up Fourier Migrations:, *in* Imaging the Earth's Interior Blackwell Scientific Publications, 272–274.

Gazdag, J., and Sguazzero, P., 1984, Migration of seismic data by phase-shift plus interpolation: Geophysics, **49**, no. 2, 124–131.

van Trier, J., and Symes, W. W., 1991, Upwind finite-difference calculation of traveltimes: Geophysics, **56**, no. 6, 812–821.

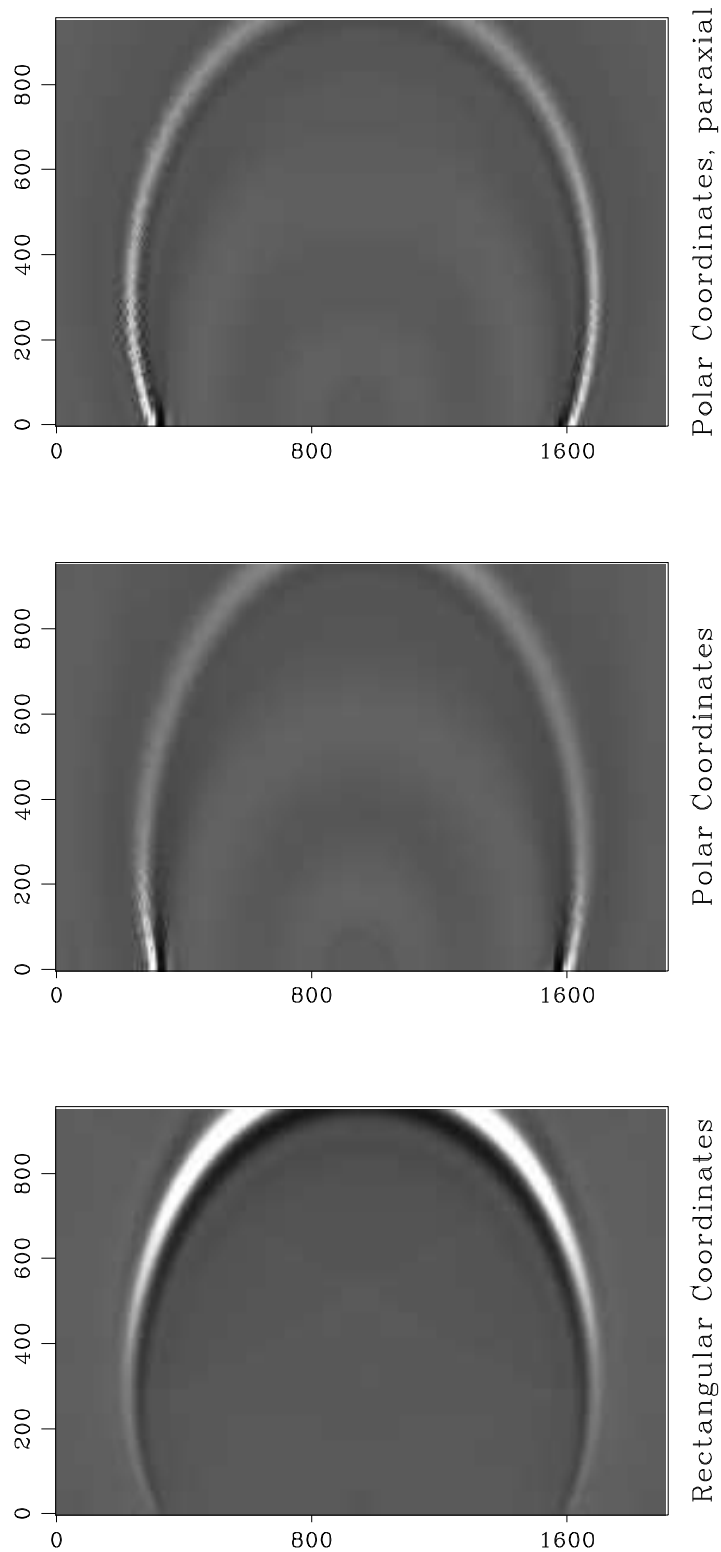


Figure 7: Modeling in a linear velocity gradient in depth. A time slice of the Green's function, depth is plotted upwards. The plot on the bottom was computed by PSPI in rectangular coordinates. The plot in the middle was computed by PSPI in a polar coordinate frame. The plot on the top was computed using the 45° wave equation in polar coordinates. dave2-over-three [CR]

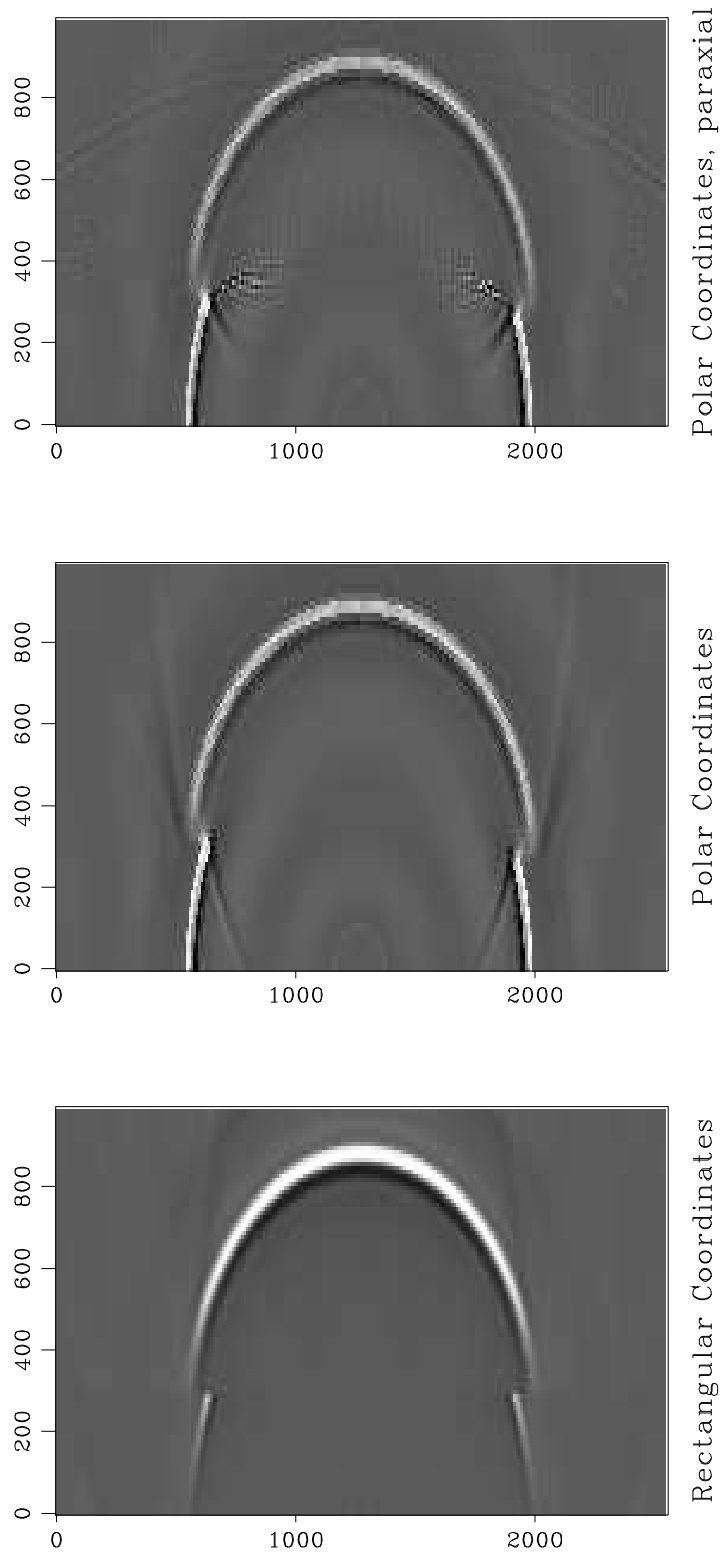


Figure 8: Modeling in a two layer model. A time slice of the Green's function, depth is plotted upwards. The plot on the bottom was computed by PSPI in rectangular coordinates. The plot in the middle was computed by PSPI in a polar coordinate frame. The plot on the top was computed using the 45° wave equation in polar coordinates. dave2-refl-three [CR]

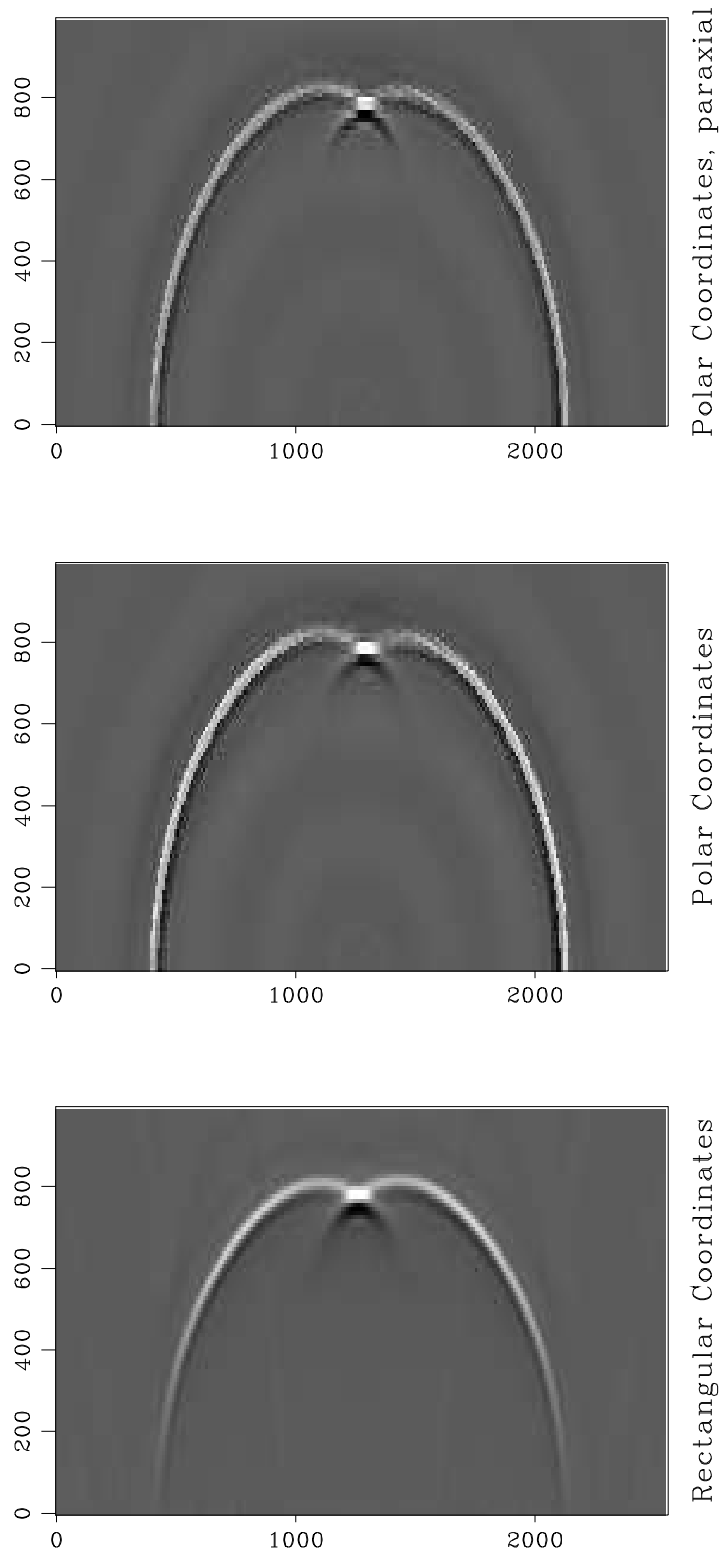


Figure 9: Modeling in medium with a Gaussian anomaly. A time slice of the Green's function, depth is plotted upwards. The plot on the bottom was computed by PSPI in rectangular coordinates. The plot in the middle was computed by PSPI in a polar coordinate frame. The plot on the top was computed using the 45° wave equation in polar coordinates. dave2-blob-three [CR]